Crystal Structure of a Complex of *Escherichia coli* Glycerol Kinase and an Allosteric Effector Fructose 1,6-Bisphosphate[†,‡]

Mats Ormö,[§,||] Cory E. Bystrom,[§,⊥] and S. James Remington*[,§,@]

Institute of Molecular Biology and Departments of Physics and Chemistry, University of Oregon, Eugene, Oregon 97403

Received July 7, 1998; Revised Manuscript Received August 18, 1998

ABSTRACT: The three-dimensional structures of *Escherichia coli* glycerol kinase (GK) with bound glycerol in the presence and absence of one of the allosteric regulators of its activity, fructose 1,6-bisphosphate (FBP), at 3.2 and 3.0 Å, are presented. The molecule crystallized in space group $P4_12_12$, and the structure was solved by molecular replacement. The models were refined with good stereochemistry to final *R*-factors of 21.1 and 21.9%, respectively. A tetrameric arrangement of monomers was observed which was essentially identical to the proposed inactive tetramer II previously described [Feese, M. D., Faber, H. R., Bystrom, C. E., Pettigrew, D. W., and Remington, S. J. (1998) *Structure* (in press)]. However, the crystal packing in this form was especially open, permitting the FBP binding site to be occupied and identified. The crystallographic data revealed a most unusual type of FBP binding site formed between two glycine-arginine loops (residues 234−236) where one-half of the binding site is donated by each monomer at the regulatory interface. The molecule of FBP binds in two mutually exclusive modes on a noncrystallographic 2-fold axis at 50% occupancy each; thus, a tetramer of GK binds two molecules of FBP. Ionic interactions between the 1- and 6-phosphates of FBP and Arg 236 were observed in addition to hydrogen bonding interactions between the backbone amide of Gly 234 and the 6-phosphate. No contacts between the protein and the furanose ring were observed. Mutagenesis of Arg 236 to alanine drastically reduced the extent of inhibition of GK by FBP and lowered, but did not eliminate, the ability of FBP to promote tetramer association. These observations are consistent with the previously characterized mechanism of FBP inhibition of GK, in which FBP acts both to promote dimer−tetramer assembly and to inactivate the tetramers.

Fructose 1,6-bisphosphate (FBP)[1] is a key intermediary metabolite, and as a glycolytic intermediate, it regulates the activity of a number of metabolic enzymes such as lactate dehydrogenase (*1*), pyruvate kinase (*2*), and glycerol kinase (*3*−*6*). Glycerol kinase (GK, EC 2.7.1.30) catalyzes the rate-limiting step in glycerol utilization, the Mg-ATP dependent phosphorylation of glycerol which yields glycerol 3-phosphate. The enzyme displays complex allosteric regulation. In addition to apparent negative cooperativity with respect to ATP concentration (*3*), FBP displays uncompetitive inhibition with respect to glycerol and noncompetitive inhibition with respect to ATP (D. W. Pettigrew, personal communication).

The activity of GK is also regulated at the transcriptional level, where glycerol 3-phosphate functions as an inducer, and in addition is inhibited by the protein IIA^{Glc} (*7*, *8*). IIA^{Glc} (M_r = 18 000, also called III^{Glc} in older literature) is the central regulatory element of the phosphoenolpyruvate: glycose phosphotransferase system, and recognizes and binds to at least 10 different target proteins, depending on its state of phosphorylation, which reflects the availability of extracellular glucose (*9*). The crystal structure of the GK−IIA^{Glc} complex in a different tetrameric form (form I) has been described (*10*). FBP and IIA^{Glc} both act to reduce v_{max}; their binding sites, however, are completely different (*11*).

Glycerol 3-phosphate can enter the glycolytic pathway after conversion to dihydroxyacetone 3-phosphate by glycerol-3-phosphate dehydrogenase. The close connection between the activity of GK and the glycolytic and other metabolic pathways seems to require glycerol kinase to be subject to strict allosteric regulation, as illustrated by the fact that cells deficient in both allosteric and transcriptional regulation of GK are killed by exposure to glycerol following growth on succinate (*12*).

The effect of FBP on GK is linked to the quaternary structure of the enzyme. Kinetic and biophysical analysis had previously indicated that at physiological concentrations,

[†] This work was supported by NIH Grant GM42618-08 to S.J.R. and a postdoctoral fellowship from the Swedish Natural Science Research Council to M.O.

[‡] The models have been deposited in the Protein Data Bank (access codes 1BOT and 1BO5 for the FBP-free form and FBP-bound form, respectively).

* Corresponding author. Phone: (541) 346-5190. Fax: (541) 346-5870. E-mail: jim@uoxray.uoregon.edu.

[§] Institute of Molecular Biology.

[||] Present address: Department of Molecular Biology, Swedish University of Agricultural Sciences, P.O. Box 590, S-751 24 Uppsala, Sweden.

[⊥] Department of Chemistry.

[@] Department of Physics.

[1] Abbreviations: FBP, fructose 1,6-bisphosphate; DTNB, dithionitrobenzoate; GK, glycerol kinase; rms, root-mean-square; ADP, adenosine diphosphate; Mg-ATP, magnesium adenosine triphosphate; Hepes, *N*-(2-hydroxyethyl)-*N*′-2-ethanesulfonic acid; EDTA, ethylenediaminetetraacetic acid.

10.1021/bi981616s CCC: $15.00
Published on Web 11/01/1998

GK exists in an equilibrium between three forms, active dimers, active tetramers, and inactive tetramers where FBP was suggested to act through stabilization of an inactive tetrameric form (*3*−*5*). The fact that there are active forms of the tetramer was indicated by the time course of desensitization toward FBP inhibition upon dilution of a concentrated enzyme solution (*4*), presumably resulting from slow dissociation of FBP-sensitive tetramers to FBP-insensitive dimers. In contrast, inhibition by IIA^{Glc} is independent of protein concentration over a wide range, and there is no evidence that the binding of IIA^{Glc} promotes the tetramer assembly reaction.

Previous structural studies (*10*, *13*) had failed to allow the FBP binding site to be identified, although an orthophosphate and sulfate binding site had been identified and was proposed to form at least part of the FBP binding site. It was further shown that orthophosphate and sulfate are inhibitors of GK (*13*). To investigate the position and nature of the FBP binding site, a new crystal form of the enzyme was obtained that permitted the analysis to proceed. In this paper, we describe the crystal structure analysis of *Escherichia coli* glycerol kinase in complex with the allosteric effector fructose 1,6-bisphosphate and describe a mutant form of the enzyme that conclusively demonstrates the observed binding site to be the physiologically relevant one.

MATERIALS AND METHODS

Materials. Restriction endonucleases and Vent polymerase for PCR were purchased from New England Biolabs. The Muta-Gene In Vitro Mutagenesis Kit was purchased from Bio-Rad Laboratories. DNA purification kits were purchased from Quiagen. The PET-28b expression system was purchased from Novagen. Oligonucleotides were purchased from Gibco, and DNA sequencing was performed on an Applied Biosystems 377 automated sequencer at the Biotechnology Laboratories at the University of Oregon.

Mutagenesis and Cloning. Kunkel mutagenesis (*14*) was carried using the Muta-Gene phagemid in vitro mutagenesis kit and the antisense primer for the R236A mutation (5′GATTGGAATAgcCGTGCCGC3′). Mutagenesis was performed in the M13mp19 phage construct RFM13 (*15*), which contains the *E. coli Hin*dIII fragment carrying the *glpK* gene. Sequencing confirmed the incorporation of the desired mutation and integrity of the gene. Double-stranded DNA was rescued and digested with *Hin*dIII. The appropriate *Hin*dIII fragment was ligated into the vector pHG165 (*16*) which had been digested with *Hin*dIII. The resulting vector was used to transform *E. coli* JM101 for expression. Difficulties in achieving expression were alleviated by recloning into PET-28b. Briefly, the ssDNA containing the R236A mutation of the *glpK* gene was amplified via PCR utilizing primers which contained restriction endonuclease sites for *Nco*I at the 5′ end (5′GAATCCATGGGCGAAAAAAAATATATCGTTGCGCTC3′) and *Xho*I at the 3′ end (5′ATCTTACTCGAGTTACATTATTCGTCGTGTTCTTCCC3′) of the final construct. The amplification products were digested and ligated into *Nco*I−*Xho*I-digested PET-28b. The resulting plasmid was used to transform *E. coli* XL1-Blue cells. Complete nucleotide sequencing of the dsDNA from a transformant confirmed the presence of the mutation and the integrity of the entire gene with the exception of the expected conversion of Thr at position 2 to Gly as a result of utilizing the *Nco*I restriction site for cloning. This plasmid was then introduced into BL21(DE3) cells for expression.

Purification, Enzyme Activity, and Kinetic Studies. Purification of the mutant glycerol kinase was carried out as previously described with minor modifications (*17*). Protein was stored as an ammonium sulfate precipitate and dialyzed against 20 mM Hepes (pH 7.0), 10 mM glycerol, 2 mM β-mercaptoethanol, and 1 mM EDTA as needed. Enzyme activity assays were performed using the previously described ADP-coupled spectrophotometric assay (*9*).

Gel Permeation Chromatography. Aliquots (1 mL) of 0.5 mg/mL GK samples in 0.1 M triethanolamine hydrochloride buffer (pH 7.0) and 2 mM glycerol, with 0, 2, and 20 mM FBP, were applied to a Sephadex G-200 column on a Pharmacia FPLC system. A flow rate of 0.3 mL/min at a pressure of <0.3 Mpa was maintained, and the effluent was monitored by UV absorption at 280 nm. The column was calibrated by using the following molecular mass standards: apoferritin (480 000 Da), γ-globulin (160 000 Da), bovine serum albumin (67 000 Da), and ovalbumin (48 000 Da). The void volume was determined with blue dextran. Retention volumes were taken as the volume at which each standard eluted from the column with the highest absorbance. A calibration curve was determined by plotting the logarithm of the molecular mass of each standard versus retention volume. Experimental molecular masses for wild type and mutant glycerol kinase were determined from the calibration curve.

Crystallization and Data Collection. Crystallization was achieved by the hanging drop vapor diffusion method. The well contained 1 mL of 1 M sodium citrate, 0.1 M Hepes (pH 7.5), and 1 mM β-mercaptoethanol. Hanging drops were prepared by mixing 5 μL of protein solution [12 mg/mL in 10 mM glycerol, 1 mM EDTA, 2 mM β-mercaptoethanol, and 20 mM HEPES (pH 7.0)] with 5 μL of a well solution and placed on coverslips over the wells. Crystals grew within 14 days at room temperature to a size exceeding 0.5 mm $\times$ 0.5 mm $\times$ 0.5 mm. Precession photography indicated that the crystals belonged to space group $P4_12_12$ or enantiomorph and were quite radiation-sensitive. Cryoprotection of the crystals for data collection was achieved by transferring the crystals to a solution of mother liquor containing 20% glycerol. Crystals were soaked in cryoprotectant for 4 h prior to freezing in a 103 K N_2 stream. FBP was introduced into the crystals by addition of 25 mM FBP to the cryoprotectant solution and extending the soak time to 16 h.

Data were collected at 103 K on an Raxis II imaging plate system using graphite-monochromated CuKα radiation generated by a Rigaku RU-100 rotating anode operated at 40 kV and 150 mA. The data were reduced using the Denzo and Scalepack programs (*18*, *19*).

Molecular Replacement and Refinement. Phases were obtained by molecular replacement using a glycerol kinase monomer with ligands and solvent removed taken from the GK−IIA^{Glc} complex structure 1GLA (Protein Data Bank code) as a search model. Rotation−function searches were calculated with the polar angle program FRFSUM (W. Kabsch, unpublished program) and translation searches with a Crowther and Blow T1 fast translation program (*20*). Rigid-body and positional refinement was carried out using

Table 1: Data Collection and Refinement Statistics

	GK ($P4_12_12$)	GK and FBP
data statistics		
no. of crystals	1	1
resolution (Å)	3.0	3.2
no. of observations	174719	188539
no. of unique observations	45067	54096
completeness (%)	81	94
R_{merge} (%)	9.0	9.2
cell parameters		
$a = b$ (Å)	168.8	169.4
c (Å)	202.7	204.7
refinement statistics		
resolution range (Å)	20−3.0	20−3.2
no. of protein atoms	7787	7818
R-factor (%)	21.9	21.1
rms deviations from ideal		
bond lengths (Å)	0.016	0.016
bond angles (deg)	2.50	2.50
B restraints (Å^2)	3.30	3.40
NCS restraints (Å)	0.54	0.56

the program TNT (*21*). Constrained noncrystallographic symmetry was used during refinement of the two chains in the asymmetric unit. Several residues (33, 276, 277, 296−298, and 402−404) differed significantly between subunits and were allowed to be refined without NCS constraints. *B* values were initially set to the Wilson *B* of the data set, and correlated *B*-factor refinement was applied in the final round of refinement. Early in refinement, a strong positive feature was observed in $F_o - F_c$ difference electron density maps which accommodated FBP. The FBP molecule is located on a noncrystallographic 2-fold axis that results in two mutually exclusive binding modes; therefore, two molecules of FBP were modeled into the density at 50% occupancy. *B*-factors for the FBP molecules were averaged over the molecule. Map interpretations and model building were carried out with the program O (*22*).

RESULTS AND DISCUSSION

Molecular Replacement Solution. GK crystallizes in space group $P4_12_12$ with cell dimensions that tend to vary from crystal to crystal of about 169 Å × 169 Å × 204 Å; therefore, each data set was collected from a single flash-frozen crystal. Data collection statistics are found in Table 1. The large unit cell dimensions suggested that a tetramer easily could fit into the asymmetric unit. However, the rotation and translation searches, conducted first with individual monomers and then with various combinations of subunits, suggested that the asymmetric unit contained only two monomers. There are two possible ways to make up the asymmetric unit of the crystal, with the rest of the tetramer being generated by a crystallographic 2-fold axis. We chose two diagonally related monomers labeled O and Z [following nomenclature previously established (*10*)] in Figure 1A as the asymmetric unit, and with this model large peaks were found in both the rotation and translation searches. The rotation function yielded a peak 5.0 standard deviations above the mean with the next largest peak at 4.3 standard deviations. If the first peak was taken as the starting model for translation searches, single peaks of typically 13.0 standard deviations about the mean yielded the *x*,*y*,*z* translations properly positioning the model in the unit cell. The next lower peaks were at 5.0 standard deviations. The starting atomic model had a crystallographic *R*-factor of 49.3% (12−4 Å resolution), but five cycles of rigid-body refinement with each monomer treated independently reduced this to 33.9%. This was followed by restrained crystallographic refinement using all the data, which reduced the *R*-factor to a final value of 24.5% for the 20−3.0 Å resolution range before model building was initiated.

Overall Structure. Final refinement statistics for the models are given in Table 1. Analysis of the quality of the final model reveals it to be acceptable given the limited resolution of the diffraction data, with only two (both Glu 84) of the 995 residues in "disallowed" regions of the Ramachandran plot and three in "generously" allowed regions. The electron density maps were not clear enough in these locations to permit a more stereochemically reasonable interpretation of the density. The overall average *B*-factor is 32 Å^2, while the average *B*-factors for glycerol and FBP are 16 and 49 Å^2, respectively. Following the indicated labeling (Figure 1A), the O−Y monomers constitute a functional dimer, whereas the FBP binding sites are located between the O−X and Y−Z interfaces. The tetramer is essentially identical to that seen in the two monoclinic crystal forms of GK (tetramer II) described in a previous paper (*13*) and is generated from the asymmetric unit by a crystallographic 2-fold axis. This result confirms the conclusions from that study that tetramer II is physiologically relevant to FBP inhibition and that tetramer I (*10*) is probably an artifact of crystallization. The only other crystal contacts in this structure, besides those at the dimer and tetramer interfaces, are in a relatively small area that includes loops containing residues 196, 277, 297, 402, and 427.

The overall loose packing in this crystal form generates a particularly interesting arrangement of protein molecules in the unit cell with extremely large channels through the crystal. The extremely high solvent content, 81% (V_M = 6.4 Å^3/Da), of this crystal form is probably responsible for the low-resolution diffraction, variability in cell dimensions, sensitivity to radiation, and high mosaicity.

The crystal packing arrangement of the $P4_12_12$ FBP−GK complex was an indication of why earlier FBP soaks with other crystal forms had failed to reveal the FBP binding site. FBP binds between two very exposed loops (residues 234−236 from each monomer), which were found to be either disordered (*10*) or involved in crystal contacts in other crystal forms and to contain bound phosphate or sulfate ions (*13*).

Except for some minor differences at the IIA^{Glc} and FBP binding sites, the overall structure of the GK monomer is essentially the same in all crystal forms reported to date. This is interesting in view of the fact that the two inhibitors, IIA^{Glc} and FBP (and its analogues), have such different binding sites and, one would assume, different modes of inhibition. The IIA^{Glc} binding site consists of GK residues 472−480 (*10*, *13*; Figure 1A), on the side of the monomer opposite from the FBP binding site (residues 234−236). This strongly suggests that both inhibitors act to stabilize the same low-activity or inactive conformation of the enzyme, but do so by independent means.

Superpositions of the FBP-free and -bound structures revealed very minor structural changes with an overall α-carbon rms fit of 0.28 Å. The largest differences were found in the FBP binding loop where the α-carbons move 0.5−1.0 Å. However, in the FBP-free form, electron density

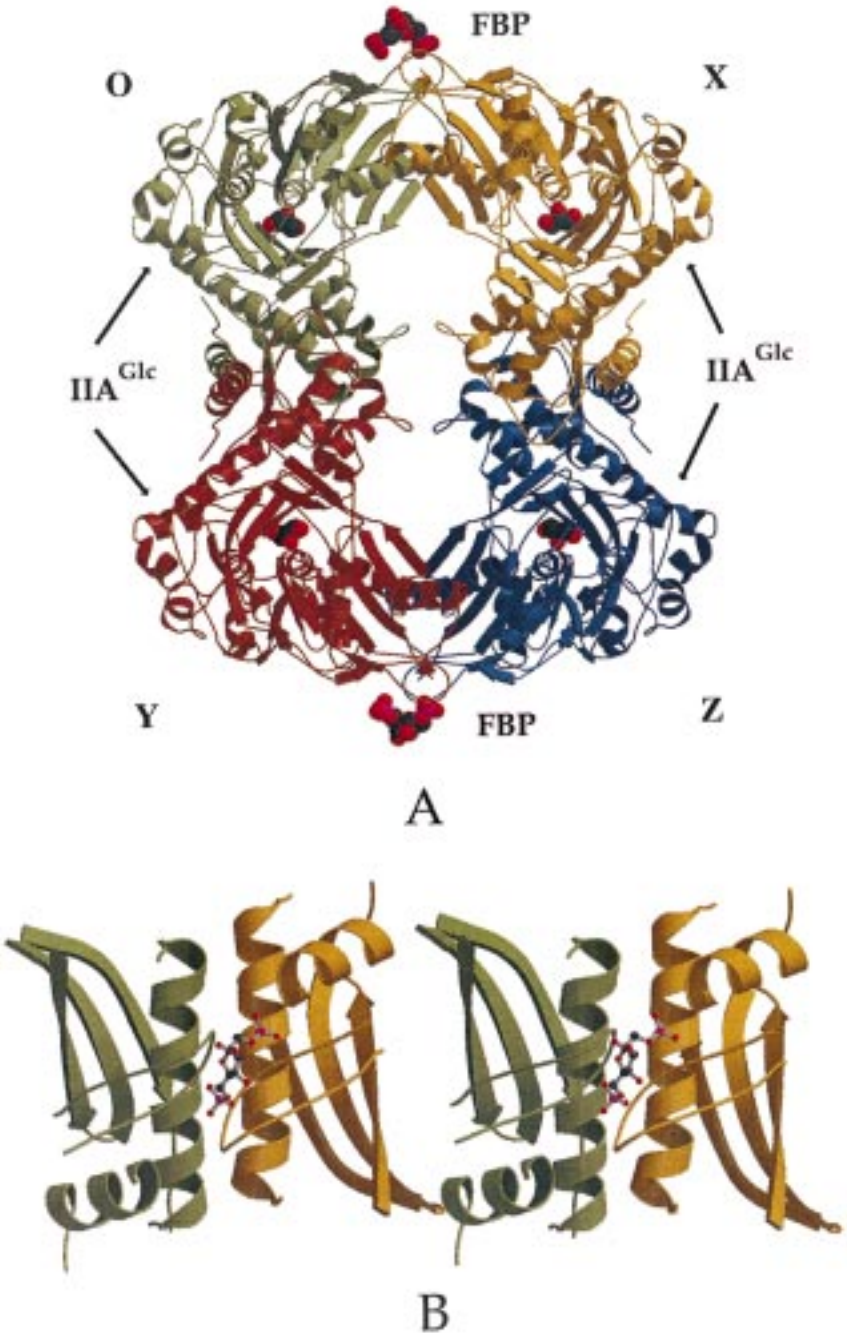

FIGURE 1: (A) MOLSCRIPT (*30*) drawing of the FBP-bound tetramer. FBP and glycerol are indicated as space filling models. The O−Y and X−Z monomers represent a functional dimer, whereas the O−Z pair constitutes the asymmetric unit of the crystal. For reference, the binding site for IIA^{Glc}, the alternative allosteric effector, is indicated. (B) Closeup schematic diagram of the O−X interface showing bound FBP in one of the two mutually exclusive binding modes.

is present at the FBP 1-phosphate binding site (described below), which might be Hepes from the crystallization buffer. A Hepes molecule was modeled into the site and appears to be an adequate interpretation of the density. Thus, buffer components might partially mimic bound FBP, as has previously been shown to be the case for phosphate and sulfate ions (K_i values of 89 and 110 mM, respectively; see ref *13*). Glycerol was found in the active sites of both structures in a configuration identical to that described for the GK−IIA^{Glc} complex (*10*). A large peak in the $F_o - F_c$ difference density map was found in the active site cleft in the area of the ATP binding site, regardless of the presence or absence of FBP. Attempts to model either citrate, ADP, FBP, or Hepes into the density were unsuccessful; therefore, nothing was modeled into this density in the final structure. Density for each of the N- and C-terminal residues was missing. No solvent molecules were added to the model due to the limited resolution of the diffraction data. The models have been deposited in the Protein Data Bank (access codes 1BOT and 1BO5 for the FBP-free form and FBP-bound form, respectively).

FBP Binding Site. The FBP binding sites are located at the O−X and Y−Z interfaces. Figure 2 shows a portion of an omit $F_o - F_c$ difference electron density map of the binding site contoured at 2σ. The electron density had the shape of an extended "W", which strongly suggested

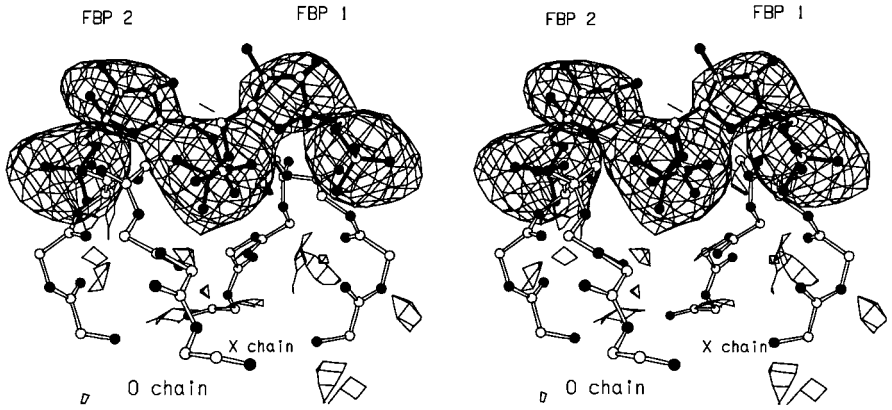

FIGURE 2: Omit map of the FBP binding site. FBP was removed from the model, and 10 cycles of constrained NCS refinement were carried out. An $F_o - F_c$ electron density map was calculated and contoured at 2σ. The coordinates for the FBP molecule are displayed in addition to the peptide backbone of residues 230−236 from the O and X chains.

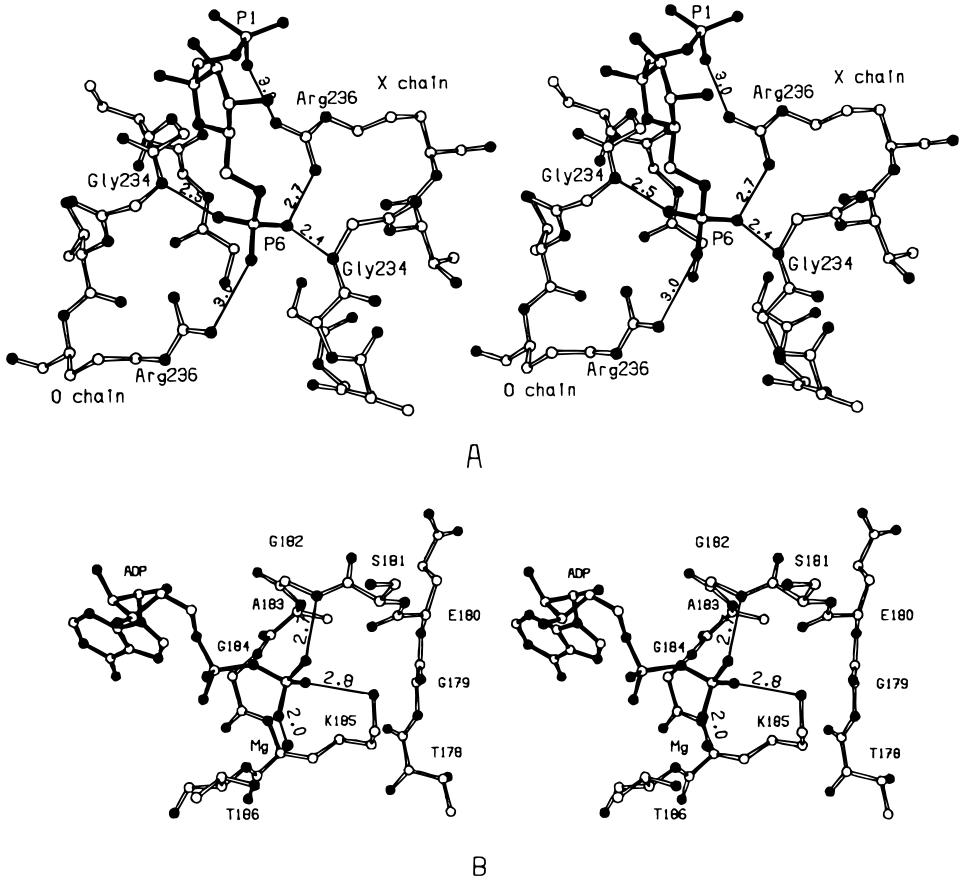

FIGURE 3: (A) Stereoview of the FBP binding loops with one of two mutually exclusive FBP molecules displayed. Hydrogen bonds and salt bridges have the approximate indicated lengths in angstroms. (B) Stereoview of a typical "P-loop" Walker type nucleotide phosphate binding motif from the myosin motor domain of *D. discoideum* (*23*) for comparison with the FBP binding loop.

orientational disorder. A noncrystallographic 2-fold axis runs through the binding site with the 6-phosphate of FBP lying on the 2-fold axis. This results in two mutually exclusive binding modes for each molecule of FBP that are equally populated, with the centrally positioned 6-phosphate common to both binding modes. A detailed representation of the FBP binding site is shown in Figure 3A. The binding site is formed by residues Gly 233, Gly 234, and Arg 236 donated from each monomer. This arrangement indicates the presence of two FBP binding sites per tetramer, which is in disagreement with the 3.5 mol of FBP bound per mole of enzyme as determined via gel filtration chromatography by Thorner and Paulus (*3*). However, the electron density maps show no convincing evidence for additional binding sites.

It is interesting that the FBP binding loop had previously been identified by sequence analysis (IGGKGGTR; *15*) as a potential "Walker-type" (GxxGxGKT/S) nucleotide phosphate binding loop, which has been seen in many ATP binding proteins; however, here the loop recognizes the phosphates of FBP. In this instance, an arginine residue (Arg 236) is substituted for the lysine of the typical P-loop. For comparison, a typical P-loop from the myosin motor domain of *Dyctostelium discoideum* (*23*) is shown in Figure 3B in roughly the same orientation as the FBP binding loop.

Arginine 236 is a key residue in FBP binding. The η-nitrogens of the guanido group of this side chain are

involved in ionic interactions with the FBP moiety in two ways. Arg 236 from one chain bridges both phosphates (1 and 6) of FBP, while Arg 236 from the other chain makes contact with the 6-phosphate on the 2-fold axis. Estimates of hydrogen bond distances are presented in Figure 3A; however, these distances must be regarded as crude because of the binding mode-generated disorder and the relatively low resolution of the crystallographic data. The only other protein contact with FBP is through the backbone amide nitrogens of Gly 234 from the O and X chains and the central 6-phosphate. An identical situation is observed at the Y−Z interface.

No contacts between the protein and the fructose moiety are observed in this structure. This is similar to what has been observed in the *Bacillus stearothermophilus* lactate dehydrogenase FBP binding site (*24*), where only one hydrogen bond is found between the furanose ring and the protein. A common characteristic for FBP binding sites tends to be localization to subunit interfaces. Examples of this are the FBP binding sites of phosphofructokinase (*25*) and fructose-1,6-bisphosphatase (*26*). The most prominent feature of FBP binding in each of these cases appears to be ionic interactions of the phosphates with the protein, leaving the rest of the FBP molecule to act as a scaffold which properly positions the phosphates. An example of this scaffolding role was demonstrated using inhibitors designed for aldolase (*27*). In that study, *N*-(ω-hydroxyalkyl) glycolamidobisphosphoric acid esters proved to be excellent inhibitors when the distance between phosphates mimicked that of FBP.

In the monoclinic GK structures (tetramer II) presented previously (*13*), a bound sulfate or phosphate molecule was identified and its nature confirmed, at the position occupied by the central 6-phosphate in the FBP-bound structure. This led to the proposal that this region of the protein formed at least part of the FBP binding site, and these studies confirm that conclusion.

Role of Arg 236 in FBP Binding and Inhibition. To demonstrate the importance of arginine 236 for the FBP binding and that the observed FBP binding site was the physiologically relevant one, this residue was mutated to alanine. Characterization of the mutagenized protein showed that FBP inhibition was essentially eliminated in comparison to that with wild type GK, at least up to 10 mM FBP (Figure 4). The K_i for FBP has increased by about 3 orders of magnitude (from 0.25 mM for the wild type to roughly 200 mM for the mutant), which would therefore be physiologically irrelevant. On the other hand, in parallel experiments, the kinetic parameters of the wild type and the R236A mutant were compared and found to be very similar (Table 2), with the mutant having only slightly lower activity.

Gel permeation experiments indicated that the R236A mutant was still able to weakly bind FBP as indicated by the small increase in the apparent molecular mass in the presence of 20 mM FBP (Table 2). The dimer−tetramer assembly reaction was clearly perturbed by the loss of Arg 236, as indicated by the lowered apparent molecular mass in the presence of FBP when compared to the wild type. This suggests that the interaction between the backbone amide of Gly 234 and the 6-phosphate of FBP is still capable of assisting in complex formation and tetramer assembly. Preliminary results from sedimentation velocity experiments

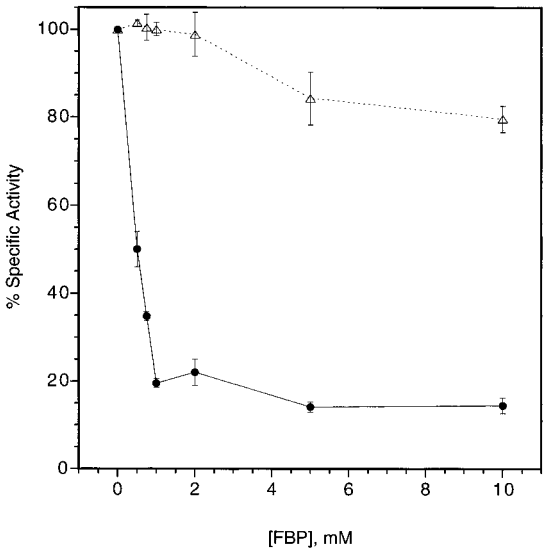

FIGURE 4: Inhibition of wild type (●) and mutant R236A (△) glycerol kinase by FBP. The specific activities of the glycerol kinases (0.4 μg/mL) were determined at pH 7.0 and 25 °C, with 2.0 mM glycerol, 2.5 mM ATP, and the indicated concentrations of FBP using the coupled assay described in Materials and Methods. Results are shown as a percentage of relative specific activity measured in the absence of FBP.

Table 2: Effect of FBP on the Properties of Glycerol Kinases

	apparent molecular mass (Da)[a]		
enzyme	0 mM FBP	2 mM FBP	20 mM FBP
R236A	109600	110600	121000
wild type	105300	199700	ND

	kinetic parameters[b]			
enzyme	v_{max} (units/mg)	$K_{M,ATP}$	$K_{M,glycerol}$	$K_{i,ATP}$
R236A	13 (10−16)	15 (3−33)	10 (6−26)	118 (16−188)
wild type	15 (14−16)	7 (5−9)	4 (2−5)	115 (60−168)

[a] Apparent molecular masses were estimated by size exclusion chromatography on Sephadex G200 as described in Materials and Methods. [b] From multiple measurements, values for the 65% confidence intervals are given. K_ms and K_i are given in units of micromolar.

conducted with an analytical ultracentrifuge support this conclusion but need to be repeated.

Role of FBP in Tetramer Assembly. The extensive kinetic and biophysical analysis by de Riel, Thorner, and Paulus (*3*−*5*) showed that FBP stabilized an inactive tetrameric form of GK by increasing the apparent dimer−tetramer association constant between 2 and 4 orders of magnitude, depending on the experimental technique used to analyze the assembly reaction. From the structure presented here, it is clear that the mechanism of stabilization of the tetramer is achieved by ionic interactions with Arg 236 and hydrogen bonding interactions of backbone amides with the phosphates at the FBP binding site, with the furanose ring providing proper spacing of the phosphates. Neutralization of the electrostatic repulsion of Arg 236 from its symmetry-related counterpart by the phosphates may also be an important aspect of FBP inhibition of GK. The bound FBP molecule bridges two monomers at each regulatory interface, stabilizing the tetrameric form of the enzyme.

The FBP binding loop of residues 230−236 was disordered and not seen in the GK−IIA^{Glc} complex (*10*), suggesting to some extent that entropic costs of ordering the

loop offset the binding enthalpy, modulating the affinity of GK for FBP. Why the loop is ordered in the FBP-free form of the crystal lattice in this study is not entirely clear, but may be due to bound buffer components as previously suggested. Recently, similar loop ordering upon FBP binding has been observed with yeast pyruvate kinase (*28*), so this may be a common feature of FBP regulation of enzyme activity.

Mechanisms of Allosteric Inhibition of GK. It is clear that inhibition of GK by IIA^{Glc} does involve long-range communication between the inhibitor binding site and the active site (*10*, *13*). Mutation of GK residues involved in IIA^{Glc} binding have pronounced effects on the catalytic activity (*13*), and IIA^{Glc} binding does not result in or depend on a change in the quaternary structure of the enzyme; that is, inhibition by IIA^{Glc} is independent of enzyme concentration.

The situtation with FBP, however, is less clear, and two possibilities need to be considered. Although previous analyses suggested that FBP stabilizes an inactive form of the tetramer that is in equilibrium with active forms of the tetramer (*3*−*5*), there is not a great deal of evidence for an active tetrameric form of the enyzme. It is therefore reasonable to consider the possibility that the tetramer assembly reaction per se could inactivate the enzyme. In the tetramer II structures described, which all contain a bound inhibitor (FBP, phosphate, or sulfate), the active site clefts face toward the center of the tetramer. If open−closed conformational changes are an essential aspect of the catalytic cycle [as seems certain, on the basis of the glycerol-induced stabilization of GK toward heat inactivation and the reduction of the number of sulfhydryls reactive toward DTNB (*3*)], it is likely that the enzyme could be inhibited by dimer−dimer interactions, preventing an open−closed conformational change. This might well be expected to be manifested in a decrease in reaction velocity rather than increased K_ms.

The kinetic analysis revealing that FBP is an uncompetitive inhibitor with respect to glycerol (D. W. Pettigrew, personal communication) indicates that FBP does not bind to the enzyme unless glycerol is also bound. In view of this, FBP action could be seen as simply "locking in" an inactive conformation of the enzyme. Thus, whether the tetramer assembly reaction alone is sufficient to inactivate the enzyme, as opposed to direct modulation of the active site structure by FBP binding, remains to be established.

In consideration of the possibility of long-range communication of the FBP binding site with the active site, the FBP-bound and -free forms were compared. There were no detectable conformational differences at the active site; however, this is inconclusive because of the relatively low resolution of the diffraction data and the absence of a bound ATP analogue. The latter consideration arises from the observed "half-of-the-sites" reactivity and negative cooperativity with respect to ATP concentration (*3*) and the possibility that FBP inhibition could be coupled to ATP binding (albeit noncompetitively). Therefore, we cannot exclude the possibility of direct communication between the active site and the FBP binding site.

Replacement of Arg 236 with alanine does result in slightly lower enzymatic activity, so this residue might be part of machinery that causes a long-range structural signal to be transmitted to the active site upon FBP binding.

Along this line of reasoning, it is interesting that the catalytic Asp 245, the putative base that deprotonates the glycerol 3-hydroxyl (*10*), is directly linked to the FBP binding site by a strand of β-sheet (residues 238−243). It seems possible that the positioning of the Asp 245 side chain could be dependent on the conformation of the FBP binding loop and that minor changes could lead to significant effects on the catalytic rate. Finally, the existence of the GK mutant G304S (centrally located in the β-sheet of the C-terminal domain), which is defective in both IIA^{Glc} and FBP regulation (*29*), suggests that both of these inhibitors do communicate with the active site via some common machinery. Regardless of the mechanistic details, both IIA^{Glc} and FBP binding appear to result in the same inactive conformation of the enzyme. However, since inhibition by IIA^{Glc} does not involve dimer−tetramer assembly, and the binding site is completely different, at least some details of inhibition by IIA^{Glc} are fundamentally different from the mechanism of FBP inhibition.

Two sets of experiments are presently underway in an attempt to distinguish between these rather different proposals for the mechanism of FBP inhibition. The tetramer structure could in principle be stabilized by introduction of disulfide bridges to form reversible cross-links at the O−X and Y−Z interfaces, and a mutant of GK that cannot assemble to a form a tetramer (S58W) has been constructed. Results of kinetic and structural studies with these mutants will be reported elsewhere.

ACKNOWLEDGMENT

We thank Karen Kallio and Patrick O'Brien for their expert technical assistance and D. W. Pettigrew for critical reading of the manuscript and helpful discussions.

REFERENCES

1. Cameron, A. D., Roper, D. I., Moreton, K. M., Muirhead, H., Holbrook, J. J., and Wigley, D. B. (1994) *J. Mol. Biol. 238*, 615−625.
2. Ashizawa, K., Willingham, M. C., Liang, C.-M., and Cheng, S.-Y. (1991) *J. Biol. Chem. 266*, 16842−16846.
3. Thorner, J. W., and Paulus, H. (1973) *J. Biol. Chem. 248*, 3922−3932.
4. de Riel, J. K., and Paulus, H. (1978) *Biochemistry 17*, 5141−5146.
5. de Riel, J. K., and Paulus, H. (1978) *Biochemistry 17*, 5134−5140.
6. Liu, W. Z., Faber, R., Feese, M., Remington, S. J., and Pettigrew, D. W. (1994) *Biochemistry 33*, 10120−10126.
7. Lin, E. C. C. (1976) *Annu. Rev. Microbiol. 30*, 535−578.
8. Pettigrew, D. W., Yu, G., and Liu, Y. (1990) *Biochemistry 29*, 8620−8627.
9. Postma, P. W., Lengeler, J. W., and Jacobson, G. R. (1993) *Microbiol. Rev. 57*, 543−594.
10. Hurley, J. H., Faber, H. R., Worthylake, D., Meadow, N. D., Roseman, S., Pettigrew, D., and Remington, S. J. (1993) *Science 259*, 673−677.
11. Novotony, M. J., Fredrickson, W. L., Waygood, E. B., and Saier, M. H., Jr. (1985) *J. Bacteriol. 162*, 810−816.
12. Zwaig, N., Kistler, W. C., and Lin, E. C. C. (1970) *J. Bacteriol. 102*, 753−759.
13. Feese, M., Faber, R. H., Bystrom, C. E., Pettigrew, D. W., and Remington, S. J. (1998) *Structure* (in press).
14. Kunkel, T. A., Roberts, J. D., and Zakour, R. A. (1987) *J. Biol. Chem. 263*, 17780−17784.

15. Pettigrew, D. W., Ma, D.-P., Conrad, C. A., and Johnson, J. R. (1988) *J. Biol. Chem. 263*, 135−139.
16. Stewart, G. S. A. B., Lubinsky-Mink, S., Jackson, C. G., Cassel, A., and Kuhn, J. (1986) *Plasmid 15*, 172−181.
17. Faber, R., Pettigrew, D. W., and Remington, S. J. (1989) *J. Mol. Biol. 207*, 637−639.
18. Otwinowski, Z., and Minor, W. (1996) in *Methods in Enzymology* (Carter, C. W., and Sweet, R. M., Eds.) Vol. 276, pp 307−326, Academic Press, New York.
19. Minor, W. (1993) *XDISPLAYF*, Purdue University, West Lafayette, IN.
20. Crowther, R. A., and Blow, D. M. (1967) *Acta Crystallogr. 23*, 544−547.
21. Tronrud, D. E. (1992) *Acta Crystallogr. A48*, 912−916.
22. Jones, T. A., and Kjeldgaard, M. O. (1998) *Methods Enzymol. 277*, 173−208.
23. Gulick, A. M., Bauer, C. B., Thoden, J. B., and Rayment, I. (1997) *Biochemistry 36*, 11619−11628.
24. Wigley, D. B., Gamblin, S. J., Turkenburg, J. P., Dodson, E. J., Piontek, K., Muirhead, H., and Holbrook, J. J. (1992) *J. Mol. Biol. 223*, 317−335.
25. Shirakihara, Y., and Evans, P. R. (1988) *J. Mol. Biol. 204*, 973−994.
26. Giroux, E., Williams, M. K., and Kantrowitz, E. R. (1994) *J. Biol. Chem. 269*, 31404−31409.
27. Ogata, H., Fukuda, T., Yamamoto, K., Yamasaki, H., Fujimoto, H., Fujisaki, S., and Kajigaeshi, S. (1990) *Biochim. Biophys. Acta 1041*, 254−256.
28. Jurica, M. S., Mesecar, A., Heath, P. J., Shi, W., Nowak, T., and Stoddard, B. L. (1998) *Structure 6*, 195−210.
29. Pettigrew, D. W., Liu, W. Z., Holmes, C., Meadow, N. D., and Roseman, S. (1996) *Methods Enzymol. 178*, 2846−2852.
30. Kraulis, P. J. (1991) *J. Appl. Crystallogr. 24*, 946−950.

BI981616S